**Atmospheric
Measurement
Techniques**

Chlorine activation by N_2O_5: simultaneous, in situ detection of $ClNO_2$ and N_2O_5 by chemical ionization mass spectrometry

J. P. Kercher[1], T. P. Riedel[1,2], and J. A. Thornton[1]

[1]Department of Atmospheric Sciences, University of Washington, Seattle, WA 98195, USA
[2]Department of Chemistry, University of Washington, Seattle, WA 98195, USA

Abstract. We report a new method for the simultaneous in situ detection of nitryl chloride ($ClNO_2$) and dinitrogen pentoxide (N_2O_5) using chemical ionization mass spectrometry (CIMS). The technique relies on the formation and detection of iodide ion-molecule clusters, $I(ClNO_2)^-$ and $I(N_2O_5)^-$. The novel N_2O_5 detection scheme is direct. It does not suffer from high and variable chemical interferences, which are associated with the typical method of nitrate anion detection. We address the role of water vapor, CDC electric field strength, and instrument zero determinations, which influence the overall sensitivity and detection limit of this method. For both species, the method demonstrates high sensitivity (>1 Hz/pptv), precision (~10% for 100 pptv in 1 s), and accuracy (~20%), the latter ultimately determined by the nitrogen dioxide (NO_2) cylinder calibration standard and characterization of inlet effects. For the typically low background signals (<10 Hz) and high selectivity, we estimate signal-to-noise (S/N) ratios of 2 for 1 pptv in 60 s averages, but uncertainty associated with the instrumental zero currently leads to an ultimate detection limit of ~5 pptv for both species. We validate our approach for the simultaneous in situ measurement of $ClNO_2$ and N_2O_5 while on board the *R/V* Knorr as part of the ICEALOT 2008 Field Campaign.
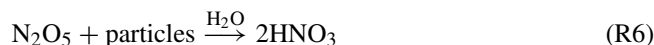
1 Introduction

Human activities of industry, transportation, and agriculture account for ~75% of global nitrogen oxide ($NO_x \equiv NO+NO_2$) emissions, and these emissions are expected to be double the 1990 values in about a decade (van

Aardenne et al., 1999; Yienger, 1999). NO_x plays a fundamental role in the troposphere's oxidizing capacity by regulating photochemical ozone production rates, and by partly controlling hydrogen oxide ($HO_x \equiv OH+HO_2$) and halogen oxide radical cycles (Logan, 1981). The regional and global scale impacts of anthropogenic NO_x emissions ultimately depend on its atmospheric lifetime, which is primarily controlled by nitric acid (HNO_3) formation during the daytime,

$$NO_2 + OH + M \rightarrow HNO_3 + M \qquad (R1)$$
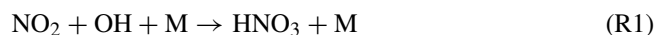
and by homogeneous and heterogeneous reactions of the nitrate radical (NO_3) and dinitrogen pentoxide (N_2O_5) at night (Reactions R2–R7).

$$NO_2 + O_3 \rightarrow NO_3 + O_2 \qquad (R2)$$

$$NO_2 + NO_3 \rightleftarrows N_2O_5 \qquad (R3)$$

$$NO_3 + VOC \rightarrow products \qquad (R4)$$

$$NO_3 + particles \rightarrow products \qquad (R5)$$

$$N_2O_5 + particles \xrightarrow{H_2O} 2HNO_3 \qquad (R6)$$

$$N_2O_5 + particles \xrightarrow{H^+,Cl^-_{aq}} ClNO_2 + HNO_3 \qquad (R7)$$

Nocturnal processing of NO_3 and N_2O_5 has been estimated to remove approximately half of NO_x, globally, and is a significant loss process for total odd-oxygen ($O_x \equiv O_3+NO_2$) (Brown et al., 2006; Dentener and Crutzen, 1993; Evans and Jacob, 2005). The chemistry involves reactions of NO_3 with a suite of diverse volatile organic compounds (VOC), and heterogeneous reactions of both NO_3 and N_2O_5 with aerosol particles(Atkinson, 2000; Jacob, 2000; Mentel et al., 1996; Noxon et al., 1980; Platt and Heintz,

Correspondence to: J. A. Thornton
(thornton@atmos.washington.edu)

1994; Wayne et al., 1991). The branching between various pathways is strongly dependent on temperature, NO_x, hydrocarbons, particle composition, and vertical mixing (Ayers and Simpson, 2006; Brown et al., 2007; Stutz et al., 2004); as such, several aspects of this chemistry remain uncertain.

Laboratory studies have conclusively shown that the reaction of N_2O_5 on chloride containing solutions and solids yields nitryl chloride ($ClNO_2$), a photo-labile chlorine atom source (Behnke et al., 1997; Finlayson-Pitts et al., 1989; Thornton and Abbatt, 2005). The relative branching between Reactions (R6) and (R7) for use in atmospheric chemistry models has essentially remained unconstrained due to a lack of in situ observations of $ClNO_2$. $ClNO_2$ is fairly unreactive at night such that given sustained production via Reaction (R7), its concentration can increase throughout nighttime. A recent theoretical study predicted $ClNO_2$ mixing ratios of up to 50 parts per trillion by volume (pptv) in polluted regions (e.g. the Long Island Sound) (Pechtl and von Glasow, 2007).

During the daytime, $ClNO_2$ undergoes photolysis by UV-VIS radiation to generate chlorine atoms and NO_2 with a clear-sky lifetime of order 30–60 min depending on season and location.

$$ClNO_2 + h\nu \rightarrow Cl + NO_2 \qquad (R8)$$

The importance of the reaction sequence (R7–R8) is twofold. First, in a NO_x-laden air mass, the photodissociation of $ClNO_2$ can initiate photochemical ozone production earlier than would otherwise occur, ultimately increasing the integral amount of ozone produced. This effect is due to the fact that Reaction (R8) goes to completion within an hour or two after sunrise, liberating chlorine atoms which react with hydrocarbons up to 10–100 times faster than does the hydroxyl radical (OH). While Cl-atoms have not been directly observed, labile sources in addition to $ClNO_2$, such as Cl_2, have been observed (Spicer et al., 1998). Regionally averaged Cl abundances have been inferred from observational analyses of hydrocarbons (Arsene et al., 2007; Cavender et al., 2008), but due to the limited spatial and temporal coverage of such measurements, the global Cl-atom source term remains largely unconstrained (Platt et al., 2004). Second, since $ClNO_2$ is not a terminal NO_x sink, production via N_2O_5 heterogeneous reaction represents a reduction, by as much as 50%, in the amount of NO_x removed during night by NO_3 and N_2O_5 chemistry, effectively enhancing the NO_x-lifetime because Reaction (R8) ultimately returns one NO_x.

Tropospheric N_2O_5 mixing ratios can vary from less than 10 pptv to above 1000 pptv (Aldener et al., 2006; Ayers and Simpson, 2003, 2006). The tropospheric N_2O_5 abundance was first inferred from long-path differential optical absorption spectroscopy (DOAS) measurements of NO_3 together with measurements of NO_2 and an assumption that NO_3, NO_2 and N_2O_5 are related by the equilibrium shown in Reaction (R3) (Heintz et al., 1996; Smith et al., 1995; Stutz et al., 2004). Recently, multiple groups have demonstrated

a difference method for in situ N_2O_5 observations, where N_2O_5 is thermally decomposed to NO_3, which is then detected by cavity ring-down spectroscopy (CaRDS) or laser-induced fluorescence (Geyer et al., 1999; Simpson, 2003; Wood et al., 2003). The contribution of ambient NO_3, which is generally small, is subtracted from the total signal measured after N_2O_5 thermal decomposition. The sum of N_2O_5 and NO_3 can also be measured as the nitrate anion, NO_3^-, by chemical ionization mass spectrometry (CIMS) using the iodide reagent ion (I^-). Indeed, this particular CIMS approach has been employed in numerous laboratory studies (Huey et al., 1995; Thornton et al., 2003) and has been demonstrated as a potential in situ method for N_2O_5 detection (Huey, 2007; Slusher et al., 2004).

Recently, we showed that $ClNO_2$ could be sensitively and selectively detected by I^- CIMS (McNeill et al., 2006), leading to the first in situ detection of $ClNO_2$ in the polluted Gulf of Mexico (Osthoff et al., 2008). Here, we describe this technique further, and demonstrate a new method that allows the detection of both N_2O_5 and $ClNO_2$ at pptv mixing ratios using the same instrument. We illustrate the instrument's performance during the initial phase of the International Chemistry Experiment in the Arctic Lower Troposphere (ICEALOT), a recent ship-based research cruise that took place March–April 2008. The unique aspects of this method include a combination of high sensitivity ($\sim 1\,Hz\,pptv^{-1}$), low background noise ($<10\,Hz$), and chemical selectivity for both $ClNO_2$ and N_2O_5. The N_2O_5 measurement is direct, i.e. the signal does not include contributions from NO_3, and it does not suffer from high and variable chemical interferences which affect the NO_3^--based detection method. Essentially, the method provides the ability to simultaneously monitor both the reactant (N_2O_5) and product ($ClNO_2$) of an atmospheric heterogeneous process, in situ, with a fixed relative calibration.

2 Instrument description

The University of Washington chemical ionization mass spectrometer (UW-CIMS), has previously been described (Wolfe et al., 2007), and is similar in concept to other field-deployable CIMS instruments (Slusher et al., 2004; Veres et al., 2008). In this section, we briefly discuss the major components and operation of the UW-CIMS with special attention paid to features allowing for detection of N_2O_5 and $ClNO_2$. A schematic of the UW-CIMS illustrating the four major components is shown in Fig. 1. These regions are: 1) ion-molecule reaction region, 2) collisional dissociation chamber, 3) octupole ion guide, 4) quadrupole mass spectrometer and electron multiplier.

2.1 Ion Molecule Reaction Region (IMR)

Ambient air, sampled by a rotary vane pump, passes through a critical orifice into a 4 cm OD electrically isolated stainless steel flow tube that serves as the IMR region. The orifice and vacuum pump maintain a constant volumetric flow rate of 2 standard liters per minute (slpm) through the sampling orifice, and a pressure of 60 torr. A commercial ^{210}Po radioactive ion source (alpha-emitter, 10 mCu), oriented perpendicular to the main sample flow axis, is located along the reaction flow tube ∼1 cm downstream of the sampling orifice. Iodide anions (I^-) are introduced to the sample stream by passing a 2.5 slpm flow of ultra high purity (UHP) N_2 that contains a trace amount of methyl iodide (CH_3I) through the ^{210}Po ion source. Neutral molecules in air react with iodide anions for ∼70 ms before exiting the IMR region.

2.2 Collisional Dissociation Chamber (CDC)

A fraction (∼10%) of the ion-molecule reaction mixture is sampled from the IMR into the collsional declustering region (CDC) by means of a second orifice biased to −65 V relative to ground. A 7 liter per second (lps) molecular drag pump is used to drop the pressure from 60 torr in the IMR to 1.5 torr in the CDC. The CDC is comprised of a series of 4 static lenses. The lenses are 2 mm thick, 4 cm OD, 1 cm ID, stainless steel discs that are spaced 6 mm from each other, and from the two orifice plates, which serve as the entrance and exit to/from the CDC. The front pair of lenses are biased to −45 V and the rear pair are biased to −25 V. The third orifice plate, which separates the CDC from the high vacuum chamber, is biased to −5.1 V to create a net electric field of −20 V/cm at 1.5 torr. This field strength is less than that typically used by our group and others to detect acyl peroxy nitrates by I^- CIMS (Wolfe et al., 2007). As discussed below, this lower field strength allows for the simultaneous detection of N_2O_5 and $ClNO_2$.

2.3 Octupole ion guide

Ions are focused through the CDC orifice plate into the fore chamber of a differentially pumped stainless steel high vacuum region. The fore chamber, pumped by a 250 lps turbomolecular pump, is maintained at 3 mtorr. Ions are focused into a narrow beam and transmitted into the quadrupole region by a custom RF-only octupole ion guide. The 4 cm long, 2 cm OD octupole ion guide, based on the designs of D. J. Tanner et al. (personal communication, 2004) at Georgia Tech., is driven by a compact RF-only power supply (2.2 MHz, 220 V p-p) designed at the University of Washington. The octupole is mounted on a fourth, and final orifice plate, which drops the pressure from 3 mtorr to 2×10^{-5} torr by means of a second 250 lps turbomolecular pump. The ion beam is focused through the orifice into the quadrupole mass selector. The two turbomolecular pumps are backed
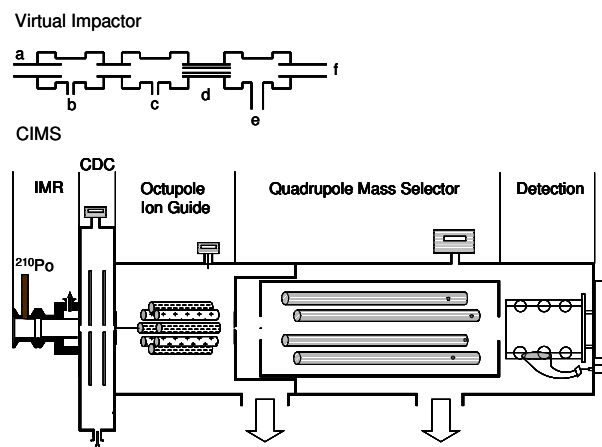

Fig. 1. Schematic of the virtual impactor and University of Washington Chemical Ionization Mass Spectrometer used while in Boulder, CO and on board the *R/V* Knorr. The virtual impactor consists of a 1 cm long, 6 mm OD inlet (**a**), N_2O_5 (**b**) and NO (**c**) addition ports, a 3 mm OD constriction (**d**), 12 m of 6 mm OD sampling line to the CIMS (**e**) and a bypass pumping line (**f**). The CIMS consists of an IMR ≡ (ion molecule region) which houses the 210 Po radioactive ion source, a CDC ≡ collisional dissociation chamber, an octupole ion guide, a quadrupole mass selector and an electron multiplier.

by molecular drag pumps, in turn backed by the same rotary vane pump which maintains the IMR region pressure and flows.

2.4 Quadrupole Mass Selection (QMS) and detection

Ions transmitted through the final orifice are mass selected using a quadrupole mass selector (QMS) from Extrel Inc. housed in a high vacuum region held at 2×10^{-5} torr. The quadrupole has 19 mm OD rods equipped with RF-only pre and post filters, and is driven by a 300 W, 1.2 MHz RF/DC power supply. The quadrupole rods are housed in a perforated stainless steel tube capped with entrance and exit lenses, and are followed by an off-axis electron multiplier detector with dynode from Extrel Inc. An MTS-100 preamp is used to convert the output pulses of the multiplier into TTL. The multiplier, preamp, and ion optics, including orifice plates and CDC lenses, are powered or biased using prepackaged Extrel Inc. power supplies.

2.5 Instrument control and data acquisition

Diagnostics monitoring and instrument control are handled via a 32-bit, 32 kHz analog-to-digital converter controlled by custom LabVIEW software on a custom rack-mounted PC. Typically, 4–20 individual mass-to-charge (*m/z*) ratios are monitored continuously while sampling ambient air. The signal at an *m/z* is determined by sending a mass command
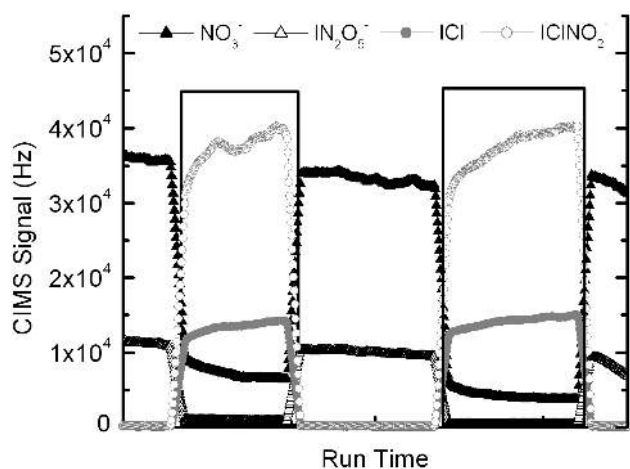
Fig. 2. UW-CIMS ion time trace showing the evolution of the ICl$^-$ (solid grey circles), I(ClNO$_2$)$^-$ (open grey circles), I(N$_2$O$_5$)$^-$ (open black triangles) and NO$_3^-$ (solid black triangles) anions when sampling a trace amount (750 pptv) of N$_2$O$_5$. The boxed regions highlight sampling periods during which the N$_2$O$_5$ flow was exposed to a wet NaCl salt bed prior to sampling by the UW-CIMS.

voltage to the RF/DC quadrupole power supply, counting the TTL preamp output for a set period per *m/z*, typically 80–250 ms, then moving to the next *m/z*. Depending on the number of individual *m/z* to monitor, this scheme leads to sampling frequencies ranging from 0.2 to 3 Hz per *m/z*.

2.6 Ion chemistry

Neglecting the role of water vapor in the ion-molecule reaction region, the ion chemistry for the detection of both N$_2$O$_5$ and ClNO$_2$ proceeds through two channels: dissociative charge transfer (Reactions R9 and R12) and cluster formation (Reactions R11 and R13). With the exception of Reaction (R11), the reaction channels described below have been demonstrated and used previously, primarily for laboratory studies (Huey, 2007; McNeill et al., 2006; Thornton et al., 2003).

$$I^- + N_2O_5 \rightarrow NO_3^- + INO_2 \tag{R9}$$

$$I^- + NO_3 \rightarrow NO_3^- + I \tag{R10}$$

$$I^- + N_2O_5 \rightarrow I(N_2O_5)^- \tag{R11}$$

$$I^- + ClNO_2 \rightarrow ICl^- + INO_2 \tag{R12}$$

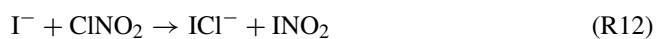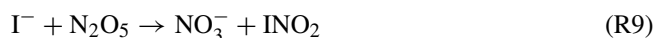$$I^- + ClNO_2 \rightarrow I(ClNO_2)^- \tag{R13}$$

Figure 2 shows a sample ion time trace obtained in the laboratory for the four products discussed above, under sampling conditions which have been optimized for the detection of the cluster anions. Initially, N$_2$O$_5$ (750 pptv) in a 2.5 slpm flow of dry N$_2$ was sampled directly into the UW-CIMS. The

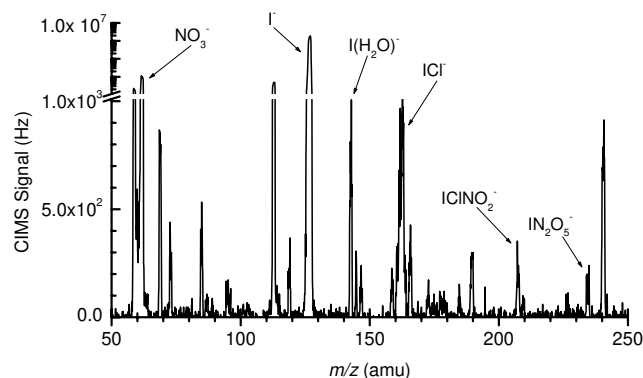**Fig. 3.** A sample mass spectrum, taken the night of 18 March 2009 while in port at Woods Hole Oceanographic Institute (WHOI). ClNO$_2$ and N$_2$O$_5$ mixing ratios were 200 and 250 ppt, respectively. All four product ions are present in addition to the two most important reagent ions, I$^-$ and I(H$_2$O)$^-$.

NO$_3^-$ and I(N$_2$O$_5$)$^-$ anions are observed in a 3:1 ratio. The boxed regions highlight the times when the N$_2$O$_5$ flow passed over a wet sodium chloride (NaCl) salt bed prior to sampling by the UW-CIMS. In addition to NO$_3^-$ and I(N$_2$O$_5$)$^-$, ICl$^-$ and I(ClNO$_2$)$^-$ are observed during these times, with the cluster anion representing 80% of the total nitryl chloride signal. Figure 3 shows a full mass spectrum, taken at Woods Hole Oceanographic Institute (WHOI) on the night of 18 March 2009. The spectrum shows all four product ions as well as the important reagent ions, I$^-$ and I(H$_2$O)$^-$. In this case, the reactive charge transfer anions are the dominant species for both N$_2$O$_5$ and ClNO$_2$, due to the dry sampling conditions and high CDC electric field of −60 V/cm. ClNO$_2$ and N$_2$O$_5$ mixing ratios were 200 and 250 ppt, respectively. The factors governing the observed branching between reactive charge transfer and cluster formation for both ClNO$_2$ and N$_2$O$_5$ are discussed below.

3 Sensitivity and selectivity

3.1 Calibrations

The true instrument sensitivity is a function of conditions both internal and external to the CIMS instrument. For example, ion transmission efficiency is affected on the short term, of minutes-hours, by temperature-dependent drifts in power supply outputs which affect static and RF potentials; and on the long term, as electron multipliers lose gain and detection efficiency decreases over the course of months to years. Air mass changes or diurnal boundary layer expansion and contraction can lead to changes in the partial pressure of H$_2$O which impacts ion chemistry. We routinely add known mixing ratios of N$_2$O$_5$ and ClNO$_2$ to the sample flow to capture such changes in instrument sensitivity. This procedure provides a calibration factor, C_f, in units of count rate per pptv

(Hz/pptv) of N$_2$O$_5$ or ClNO$_2$ sampled, that is then interpolated onto the measurement time base and used to convert instantaneous count rates into absolute mixing ratios.

Well-quantified, highly reproducible, and commercially available sources of N$_2$O$_5$ and ClNO$_2$ do not exist. We use a combination of generation and quantification methods to develop confidence in the calibration sources we apply in the field. During ICEALOT 2008, N$_2$O$_5$ was delivered to the sampling inlet for calibration purposes, one to two times per day, by passing a small flow of N$_2$ over pure, solid N$_2$O$_5$ maintained at 200 K. Two types of additions were performed: one while overflowing the inlet with dry zero air, and one by adding the N$_2$O$_5$ directly to moist ambient air. In general, calibrations were conducted between 01:00–04:00 p.m. local time. This time was chosen to insure that the atmospheric N$_2$O$_5$ and ClNO$_2$ signals had decayed completely in the morning hours but also to allow ample time for the inlet cleaning and replacement before sunset. The NOAA CaRDS instrument, sampling from the same inlet manifold as the UW-CIMS, used these additions primarily to assess inlet transmission. For the purpose of this campaign, a goal of which was to test our N$_2$O$_5$ detection capability, we relied on the NOAA CaRDS instrument to determine the N$_2$O$_5$ concentration being delivered to the UW-CIMS inlet during these calibrations. We then used this known N$_2$O$_5$ concentration, typically a single value between 1–5 ppbv, to generate a C_f for the UW-CIMS based on the observed signal at the I(N$_2$O$_5$)$^-$ m/z. Figure 4 shows the resulting plots of signal (Hz) versus N$_2$O$_5$ mixing ratio sampled in relatively dry air (RH$\sim$20%). The slope of linear least squares fit to the data yield a calibration factor of 0.75 Hz/pptv. An example of a calibration performed during the deployment is shown and discussed in the section on field performance.

We calibrate to ClNO$_2$ by passing a known mixing ratio of N$_2$O$_5$ in either a relatively dry N$_2$ flow or ambient air over a wet NaCl bed, which is dispersed along the inner walls of a 20 cm length of 13 mm OD tubing. The mixing ratio of ClNO$_2$ eluting from the salt bed is calculated from the observed amount of N$_2$O$_5$ lost when passing through the salt bed and the known ClNO$_2$ yield (100%) from the reaction of N$_2$O$_5$ on NaCl (Behnke et al., 1997; Finlayson-Pitts et al., 1989; McNeill et al., 2006). For ClNO$_2$ calibrations, the ion counts are plotted against the amount of N$_2$O$_5$ lost, as in Fig. 4. The ClNO$_2$ data in Fig. 4 were obtained using the same flow conditions as for the N$_2$O$_5$ calibration described above.

The difficulty with using the equilibrium vapor pressure over solid N$_2$O$_5$ as a CIMS calibration source is that the N$_2$O$_5$ solid is subject to contamination, which results in unknown changes in the vapor pressure on a weekly, if not daily timescale. Without an absolute calibration, such as the known NO$_3$ absorption cross-section available to cavity ring-down techniques, abrupt (or gradual) changes in trap-output are undesirable. Furthermore, temperature control of the cold-bath must also be precise given that the vapor pres-
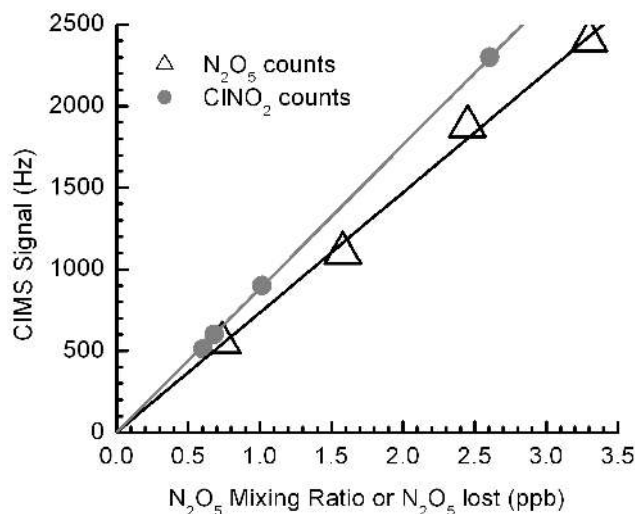

Fig. 4. UW-CIMS signal (Hz) vs mixing ratio (ppbv) for N$_2$O$_5$ (triangles) and ClNO$_2$ (circles) at the I(N$_2$O$_5$)$^-$ and I(ClNO$_2$)$^-$ cluster anion masses, respectively. The size of the points corresponds to the 1σ deviation of the points used in the average. The N$_2$O$_5$ mixing ratio was determined using the NOAA CaRDS. The ClNO$_2$ mixing ratio is assumed to be equal to the amount of N$_2$O$_5$ which reacts over a wet NaCl salt bed and is plotted against the reacted N$_2$O$_5$ concentration. The slopes of the linear regressions provide the UW-CIMS sensitivities to each cluster anion.

sure in equilibrium with the solid changes by 30–50% per degree K, and routine calibrations require dry ice or liquid nitrogen to maintain the trap cold-bath which is not ideal for long field deployments. Our preferred method for independent calibration of the UW-CIMS to N$_2$O$_5$ in future field deployments is to deliver the output from a custom PFA-Teflon flow reactor in which N$_2$O$_5$ is continuously produced from the well known reaction of NO$_2$ with O$_3$, i.e. Reactions (R2–R3). This N$_2$O$_5$ source is described in detail elsewhere (Bertram et al., 2009).

3.2 Factors affecting sensitivity

Fundamentally, the sensitivity and linearity of a CIMS method depends on the rate of product ion formation, the ion-molecule reaction time, and the ion transmission and detection efficiencies. Ideally, the product ion formation rate is maximized by using high densities of a reagent ion which reacts at the collision limit with the analyte of interest to produce detectable count rates (Hz) of a unique product ion in a short interaction time. A short interaction time ensures a small extent of reaction and thus that the product ion abundance remains linearly proportional to the analyte concentration. For a more complete discussion of these issues, we refer the reader elsewhere (Harrison, 1983). Here, we focus on two factors which affect the sensitivity of our I$^-$ CIMS to ClNO$_2$ and N$_2$O$_5$ via the iodide cluster channels
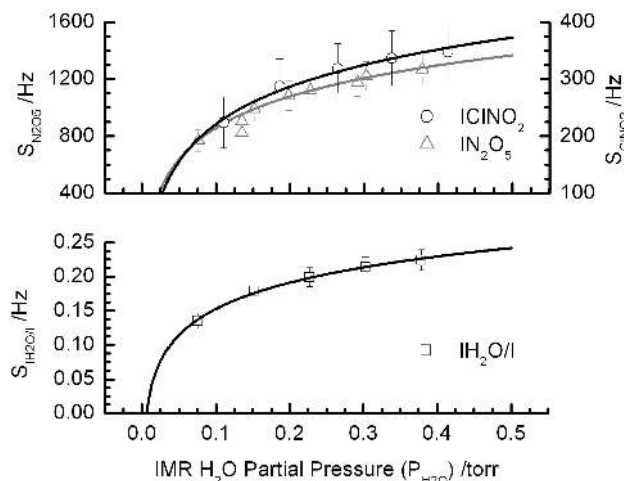
Fig. 5. Upper Panel: UW-CIMS cluster anion signal dependence on the ion molecule region (IMR) water partial pressure (P_{H_2O}). Lower Panel: the iodide-water (IH$_2$O$^-$) cluster anion signal, normalized to the iodide reagent ion signal (I$^-$).
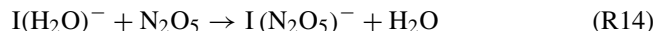
(Reactions R11 and R13): water vapor mediated cluster formation and collisional dissociation in the CDC.

In sampling humid ambient air, iodide ions form clusters containing one or more water molecules, as do many of the analyte ions produced during the chemical ionization process. The formation of such complexes can enhance sensitivity by stabilizing reactive complexes, or, as is more often the case, such complexes can degrade sensitivity by reducing the reactivity of the reagent ion and/or by distributing the analyte ion of interest among several m/z thus decreasing the signal-to-noise (S/N). For this latter reason, a number of CIMS instruments employ a CDC to increase the S/N, by collapsing the analyte ion water cluster distribution into a single m/z representative of the parent ion mass. We illustrate below that both aspects are important.

3.2.1 Water vapor mediated cluster formation

Figure 5 shows the water vapor dependence of the I(ClNO$_2$)$^-$ and I(N$_2$O$_5$)$^-$ signals. To obtain this data, a constant mixing ratio of 2 ppb of N$_2$O$_5$ and ∼1 ppb of ClNO$_2$ were delivered to the UW-CIMS inlet as described below, while a humidified flow of N$_2$ was delivered directly to the IMR region via a separate length of tubing and orifice so that the results were not affected by humidity-dependent losses of N$_2$O$_5$ on the inlet tubing walls. The experiments were conducted with a CDC electric field strength of −60 V/cm (at 1.5 torr) that we use to simultaneously detect acyl peroxy nitrates, N$_2$O$_5$, and ClNO$_2$ in the field. The signals at both the N$_2$O$_5$ and ClNO$_2$ iodide clusters increase rapidly at low water concentrations and become independent of water vapor at approximately 0.3 torr water vapor pressure, P_{H_2O}, in the IMR region. Due to the moist salt bed used to pro-

duce ClNO$_2$, we were unable to achieve $P_{H_2O} < 0.1$ torr in the IMR. Clearly, the formation of the N$_2$O$_5$ and ClNO$_2$ clusters is facilitated by water vapor implying that the I(H$_2$O)$^-$ cluster likely becomes an important additional reagent ion for production of I(ClNO$_2$)$^-$ and I(N$_2$O$_5$)$^-$

$$I(H_2O)^- + N_2O_5 \rightarrow I(N_2O_5)^- + H_2O \qquad (R14)$$

$$I(H_2O)^- + ClNO_2 \rightarrow I(ClNO_2)^- + H_2O \qquad (R15)$$

The behavior observed here for the N$_2$O$_5$ and ClNO$_2$ iodide clusters is remarkably similar to that exhibited by acyl peroxy radicals (Slusher et al., 2004). Under minimal declustering, i.e. E < −5 V/cm in the CDC, the ratio of I$^-$ to I(H$_2$O)$^-$ signals is approximately 1:1 to 1:2. Higher order water clusters, such as I(H$_2$O)$_2^-$ and I(H$_2$O)$_3^-$, are detected, but are less than 25% and 10%, respectively, of the I(H$_2$O)$^-$ cluster signal. Thus, we presume that both I$^-$ and I(H$_2$O)$^-$ are the most important reagent ions. Indeed to obtain excellent agreement between the NOAA-CaRDS N$_2$O$_5$ measurements and the UW-CIMS N$_2$O$_5$ measurements, we must scale our I(N$_2$O$_5$)$^-$ cluster signal by the I(H$_2$O)$^-$/I$^-$ ratio to take into account fluctuations in ambient water vapor that affect our sensitivity. While the nitrate anion does cluster with water, producing NO$_3$(H$_2$O)$^-$, there is no evidence that the iodide clusters of ClNO$_2$ or N$_2$O$_5$ form water clusters under the sampling conditions reported in this study.

3.2.2 Collisional dissociation in the CDC

While the sensitivity to ClNO$_2$ and N$_2$O$_5$ at their respective iodide clusters is enhanced by the presence of water vapor, it is degraded by collisional dissociation in the CDC. Thus, we strike a balance in the operation of the CDC. The CDC electric field must be strong enough to dissociate water molecules associated with the analyte ions of interest to maintain a high S/N at the cluster-ion m/z. However, the field strength must be weak enough to allow the survival of the I(ClNO$_2$)$^-$ and I(N$_2$O$_5$)$^-$ clusters. In practice, there are often other species of interest for detection, such as acyl peroxy nitrates, the product ions of which may cluster with water more strongly than the iodide clusters of N$_2$O$_5$ and ClNO$_2$. Thus, it may be necessary to choose a CDC electric field strength that does not favor maximum sensitivity to N$_2$O$_5$ and ClNO$_2$ via their iodide clusters if other species are to be measured.

The overall sensitivity and detection limit for a particular species is improved by producing a single ion for detection. By knowing the branching ratio between the reactive charge transfer and cluster ion formation, the sensitivity and detection limit of the CIMS can be further optimized. To obtain an estimate of the branching between Reactions (R9) and (R11), and between (R12) and (R13) in the IMR at 60 torr, we examined the ratios of I(ClNO$_2$)$^-$ to ICl$^-$ signals and of I(N$_2$O$_5$)$^-$ to NO$_3^-$ and NO$_3$(H$_2$O)$^-$ signals as a function of electric field strength in the CDC and the results for N$_2$O$_5$ are plotted in the lower panel of Fig. 6. With relatively

moist N$_2$ sample or ion source flows, I(N$_2$O$_5$)$^-$ approaches up to ~75% of the total measured N$_2$O$_5$ signal {I(N$_2$O$_5$)$^-$ + NO$_3^-$ + NO$_3$(H$_2$O)$^-$} as the CDC field strength is lowered below -20 V/cm at 1.5 torr (upper panel, Fig. 6). The cluster anion, I(N$_2$O$_5$)$^-$, remains the dominant ion signal up to -40 V/cm, but at high CDC electric fields (<-70 V/cm), the nitrate anion signal dominates. It should be noted that the cluster product ions dissociate in the CDC so the relative signals detected after the CDC provide only lower limits to the true branching of the ion-molecule reactions occurring upstream of the CDC. Other CIMS instruments using a CDC typically employ electric fields of -60 to -80 V/cm but at lower pressures (Slusher et al., 2004; Veres et al., 2008) leading to even larger collisional dissociation energies and thus would require smaller potentials relative to ground for detection of the clusters than those shown here. In addition, the affect of water vapor on product ion branching ratios can be inferred from the mass spectrum presented in Fig. 3 in the context of the effect of CDC potentials just described. In Fig. 3, the CDC electric field strength is -60 V/cm, however the ambient sample flow was fairly dry (RH~30%) and thus the dissociative charge transfer anions, NO$_3^-$ and ICl$^-$, are more abundant than expected based solely on the CDC electric field strength. The branching between charge transfer and cluster formation reactions are likely pressure dependent, and thus the IMR pressure also likely affects the absolute branching given that the cluster channels are probably enhanced by third-body stabilization of the complexes. This issue deserves further study and has implications for the ability of other CIMS instruments with different IMR and CDC pressures to use this reaction scheme.

3.3 Specificity and instrumental zero determinations

In a complex matrix such as air, signal at some m/z cannot always be uniquely attributed to a specific compound. Chemical ionization provides a degree of specificity given that many possible ion-molecule reactions are either kinetically or thermodynamically prohibited from occurring. Thus, the appropriate choice of a reagent ion can greatly improve specificity. N$_2$O$_5$ and ClNO$_2$ also have certain chemical properties which can be utilized to enhance the inherent specificity of the CIMS method. First, both N$_2$O$_5$ and ClNO$_2$ thermally decompose around 425 K (Zhu and Lin, 2004). Second, at temperatures near 298 K, N$_2$O$_5$ exists in a dynamic equilibrium with NO$_3$ and NO$_2$. NO$_3$ reacts rapidly with NO to form NO$_2$

$$NO_3 + NO \rightarrow 2NO_2 \qquad (R16)$$

Thus, addition of high concentrations of NO to sample air near room temperature should effectively titrate both N$_2$O$_5$ and NO$_3$ from the sample air (Fuchs et al., 2008). Third, chlorine has two abundant isotopes, ^{35}Cl and ^{37}Cl, naturally present at ~3:1, respectively. Thus, the I(ClNO$_2$)$^-$ cluster will appear at both 207.9 and 209.9 m/z in a ratio that should
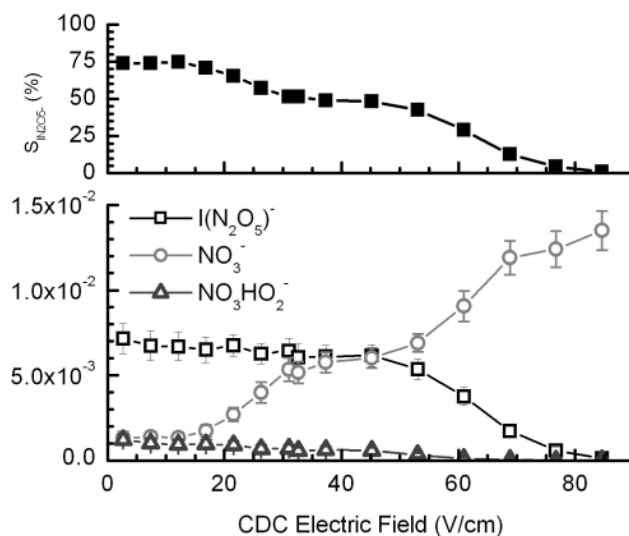

Fig. 6. Upper Panel: relative IN$_2$O$_5^-$ cluster anion signal (%). Lower Panel: N$_2$O$_5$ anion signal (IN$_2$O$_5^-$, NO$_3^-$, NO$_3$H$_2$O$^-$) dependence on the CDC electric field.

match the natural isotopic abundance for chlorine. We use all of these qualities to ensure specificity in the N$_2$O$_5$ and ClNO$_2$ measurements. We assume that it is highly unlikely there exists chemical species that have m/z identical to N$_2$O$_5$ and ClNO$_2$, that cluster with the iodide ion, and that have the same chemical properties described above. Recent field tests suggest this assumption is valid.

To account for sources of signal at the I(N$_2$O$_5$)$^-$ and the I(ClNO$_2$)$^- m/z$ that are not due to N$_2$O$_5$ or ClNO$_2$, i.e. sources of background noise, we perform routine "zero" determinations in which N$_2$O$_5$ and ClNO$_2$ are scrubbed from ambient air and the residual signal is recorded. This background signal has two main sources: internal electronic noise and interferences, the latter of which are ions having m/z within the mass resolution of the m/z of the N$_2$O$_5$ and ClNO$_2$ iodide clusters. Our zero determinations include both short additions of high concentrations of NO (~1 ppm) to the sampling manifold to titrate N$_2$O$_5$ in a long-residence time tube, and sampling ambient air through a 30 cm long, 13 mm OD stainless steel tube filled with stainless steel wool and heated to 450 K. The air exiting the hot metal tube passes through a 20 cm length of 6 mm OD tubing and thus likely cools back to near ambient temperature prior to entry into the UW-CIMS. This latter method, with its high surface area of hot metal, efficiently scrubs NO$_3$ and Cl-atoms released by thermal decomposition of N$_2$O$_5$ and ClNO$_2$ whereas the NO addition will only scrub N$_2$O$_5$.

Instrument zeros performed through a hot metal thermal dissociation tube are simple, but must be carefully examined. For example, it is possible that an interfering species is also lost in the hot metal tube or that the composition of the air is significantly changed to affect the overall sensitivity. Both

Table 1. Table 1: Summary of UW-CIMS performance for simultaneous, in situ detection of N$_2$O$_5$ and ClNO$_2$ during ICEALOT.

Species	Ion	Sensitivity (Hz/pptv)	Background (Hz)	Detection Limit[a] (pptv) (1 s/1 min)	Zero Uncertainty[b] (pptv)
N$_2$O$_5$	I(N$_2$O$_5$)$^-$	0.93±0.2	2.1±2	11.0/2.7	2.3
N$_2$O$_5$	NO$_3^-$	4–40[c]	200–4000[c]	<2[c]	50–100[c]
ClNO$_2$	I(ClNO$_2$)$^-$	1.18±0.15	2.7±2.3	13.0/3.0	2.0

[a] Mixing ratio which yields an instantaneous signal-to-noise ratio of 2:1. This theoretical value assumes the background count rate is known with absolute certainty.

[b] Based on 1σ variation between adjacent background measurements. This value is a more realistic measure of the lowest detectable mixing ratio. See text for details.

[c] Sensitivity and background values for NO$_3^-$ m/z covaried unpredictably, and thus these values are highly uncertain.

scenarios lead to an uncertainty in the true background. We have observed that the P_{H_2O} in the IMR is routinely lower during zero determinations than during ambient sampling, implying a different sensitivity during zero determinations (Fig. 5). To account for such sensitivity differences, we use I(H$_2$O)$^-$ and I(H$_2$O)$^-$ signals as indicators of P_{H_2O} and the sensitivity behavior shown in Fig. 5 to scale our measured background signal accordingly. This leads to an average background of 3±2 pptv for both N$_2$O$_5$ and ClNO$_2$.

3.4 Detection limits

The lowest concentration that gives rise to a signal which can be statistically differentiated from the instrumental background is termed the detection limit. It is a function of the instrumental sensitivity, background noise, and averaging time. A useful threshold for a statistical definition of a detection limit is the concentration at which the signal-to-noise ratio (S/N) is 2. Discrete ion counting follows Poisson statistics, thus the expected random variation about a mean count rate goes as the square root of the count rate. The signal-to-noise ratio can be calculated via

$$\frac{S}{N} = \frac{C_f\,[X]\,t}{\sqrt{C_f\,[X]\,t + 2\,Bt}} \qquad (1)$$

where the numerator provides the total number of counts produced during a given integration period, t, while sampling air with a mixing ratio, $[X]$, of N$_2$O$_5$ or ClNO$_2$, and with a calibration factor, C_f. The denominator represents the total noise associated with such a measurement which comes from the scatter about the sum of the count rate associated with the signal and the underlying background count rate, B.

Under moist ambient conditions at Earth's surface, i.e. RH >50% and T >280 K, the C_f for N$_2$O$_5$ and ClNO$_2$ at the iodide clusters are 1.1 and 1.3 Hz/pptv, respectively, and background count rates are 2 and 3 Hz, respectively. These parameters and Eq. (1) yield detection limits for N$_2$O$_5$ and ClNO$_2$ of 11 and 13 pptv for a one second measurement. These values improve with the square root of the averaging time to <2 pptv for a 1-min average. However, there is a limit

to which time averaging can improve the S/N. The ability to distinguish signal from the background depends on the uncertainty in the background value which can be approximated as the point-to-point variation in the values determined by individual zero determinations as described above. During a recent field campaign the 1σ variation in the background count rate measurements was 2.5 Hz for N$_2$O$_5$ and ClNO$_2$, respectively, which is equivalent to 2.3 and 2.0 pptv using the above C_f.

3.5 Accuracy and precision

Ultimately, we expect the accuracy of our reported N$_2$O$_5$ and ClNO$_2$ mixing ratios will be largely determined by uncertainty in the NO$_2$ cylinder and O$_3$ concentration measurement. As described in Bertram, et al. (2009), the output of our continuous-flow N$_2$O$_5$ source agrees with the predicted values to within the ±20% uncertainty in the NO$_2$ cylinder concentration, O$_3$ mixing ratio measurement, and plug-flow estimated reaction time in the synthesis volume. Other sources of inaccuracy include unaccounted for fluctuations in sample flow rates, IMR pressure, ambient water, instrument trailer temperature, and inlet transmission efficiency. We actively control IMR pressure and sample flow rates to better than 1%, we use short transit times through sample tubing (250 ms) to minimize wall interactions and chemistry, and we employ daily standard addition calibrations and inlet transmission tests to assess drift on this timescale. On shorter timescales, we rely on normalization of ion count rates to the total I$^-$ and I(H$_2$O)$^-$ to capture changes in sensitivity due to changes in ion transmission and ambient water vapor. Note, the sensitivity varies by only 0.25% per percent change ambient water vapor mixing ratio when P_{H_2O} >0.2 torr. It is only in regions where P_{H_2O} <0.15, and changing on timescales faster than can be normalized by the I(H$_2$O)$^-$ (i.e. >0.5 Hz) that such contributions to uncertainty become important. Indeed, our instrument calibration factor, C_f, for N$_2$O$_5$ and ClNO$_2$ varied by less than 25% (1σ) across the entire 40-day sampling campaign of ICEALOT (see Table 1) without correcting for variations in water vapor mixing ratios.

Thus, for hourly or longer time averages, across which we will have a well-calibrated knowledge of instrument sensitivity and background, we estimate an accuracy of $\pm 20\%$ for ClNO$_2$ and N$_2$O$_5$ mixing ratios well above 5 pptv.

We expect that the precision of our N$_2$O$_5$ and ClNO$_2$ observations is governed largely by counting statistics as we have already demonstrated for our acyl peroxy nitrate measurements using adjacent differences of high time resolution measurements of a calibration source (Wolfe et al., 2007). The 1σ relative precision under counting statistics is $S/\sqrt{S}$ where S is the signal count rate. For a 1 s integration and 100 pptv N$_2$O$_5$ or ClNO$_2$, we estimate a precision of 10% and 7.5%, respectively under moist conditions. This precision improves with the square root of the integration time. Generally, atmospheric variability is large enough, even on 60-s timescales to be the dominant source of point-to-point variability. Indeed given the poor vertical mixing near the surface at night, very large relative changes in concentrations are possible on short timescales.

4 Field performance

We recently deployed the UW-CIMS instrument aboard the Research Vessel (*RV*) *Knorr* as part of the International Chemistry in the Arctic Lower Troposphere (ICEALOT) campaign. The measurement campaign ran from 19 March–24 April, 2008 as the ship left Woods Hole, MA and traveled from the Long Island Sound to Rekjavik, Iceland via Tromso, Norway. For more information on the goals and measurement suite during this campaign please visit: http://saga.pmel.noaa.gov/Field/icealot/. Our goal was to provide high quality measurements of ClNO$_2$ and to test the performance of our N$_2$O$_5$ measurement technique side-by-side with the NOAA cavity ringdown spectrometer (CaRDS) instrument (Brown et al., 2002). Table 1 summarizes instrument performance during this campaign.

Prior to deployment, the UW-CIMS instrument and the NOAA CaRDS instrument made ambient measurements in Boulder, CO as part of the integration of the instruments into the shipping container that housed them on the *RV Knorr*. The inlet configuration, shown in Fig. 1, for sampling both in Boulder, CO and on the Knorr is a virtual impactor, consisting of N$_2$O$_5$ and NO addition ports, a reducer, and a 12 m length of 6 mm OD PFA tubing into the sea container. Ambient air is sampled at $\sim$11 slpm through a 1 cm length of 6 mm OD PFA tubing inlet (a) on the front end of a custom built virtual impactor (f). Standard addition ports for N$_2$O$_5$ (6 mm, b) and NO (3 mm, c) are tied into the main sampling line via PFA fittings. Immediately following the NO addition port is a constriction (d) which serves to drop the sampling line pressure to $\sim$300 torr. A 12 m length of PFA tubing is used to transport the gas from the top of the sampling tower to the sea container (e) where it is split $\sim$1 m from the end to
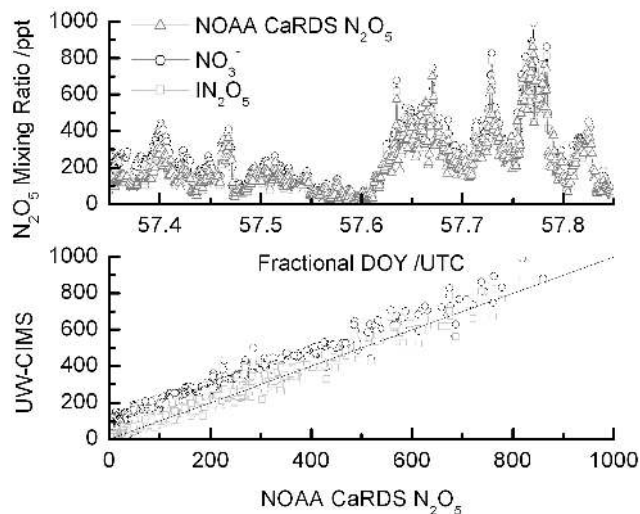

Fig. 7. Upper Panel: the N$_2$O$_5$ mixing ratio for 26 February, 2008, as measured by the NOAA CaRDS (triangles), the I(N$_2$O$_5$)$^-$ cluster (squares) and NO$_3^-$ (circles). Lower Panel: a comparison between the I(N$_2$O$_5$)$^-$ cluster (squares) and NO$_3^-$ anion (circles) with the NOAA cavity ringdown measurement, respectively. The solid black line is a 1:1 ratio.

allow the UW-CIMS and NOAA CaRDS to sample from the same inlet simultaneously.

The top panel of Fig. 7 shows N$_2$O$_5$ mixing ratios measured by the UW-CIMS and the NOAA CaRDS in Boulder, CO the night of 26 February 2008. N$_2$O$_5$ mixing ratios increase throughout the night to 800 pptv, remain elevated throughout the night and then decay in the morning following sunrise likely due to the photolysis of NO$_3$ and its reaction with NO. For comparison we have included N$_2$O$_5$ mixing ratios determined from the signal at the nitrate ion mass (i.e. Reaction R9) where we have used zero measurements determined only from NO additions. If we use zero measurements obtained from the hot stainless steel tube, the lack of agreement between the NO$_3^-$ and the I(N$_2$O$_5$)$^-$ derived N$_2$O$_5$ mixing ratios worsens. The lower panel shows a point-by-point comparison of the data with the UW-CIMS N$_2$O$_5$ mixing ratio derived from I(N$_2$O$_5$)$^-$ and NO$_3^-$ plotted versus that from the NOAA CaRDS. The slope of a linear least squares fit for I(N$_2$O$_5$)$^-$ is 1.02 with an R^2 of 0.990. The slope of the line changes by 2% when the intercept is allowed to vary from zero. The slope of a linear least squares fit for NO$_3^-$ is 1.20 with an R^2 of 0.967 when forced through zero. The slope of the line changes by 20% when the intercept is allowed to vary from zero, resulting in a positive offset of 58 pptv. Even larger swings in sensitivity and background were observed at the NO$_3^-$ m/z during the entire ICEALOT campaign (see Table 1 and Fig. 7). A more detailed comparison of the NOAA CaRDS and UW-CIMS N$_2$O$_5$ measurements from ICEALOT is warranted. However, it is clear that the I(N$_2$O$_5$)$^-$ cluster ion more accurately reflects the true
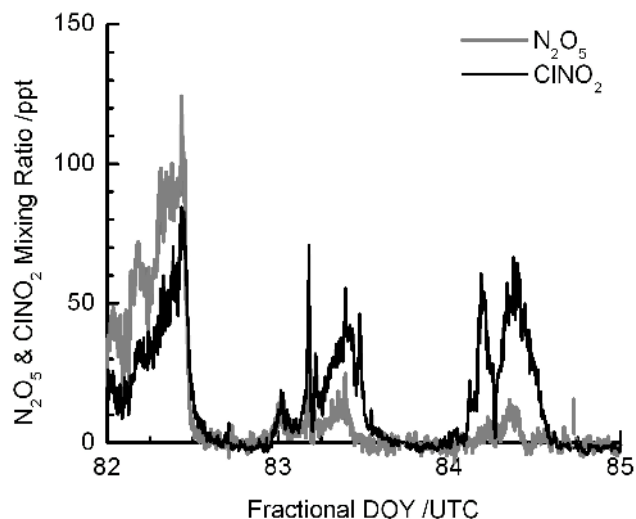
Fig. 8. The ClNO₂ (black) and N₂O₅ (grey) mixing ratios measured from 22 March (DOY 82) through 24 March 2008 during the ICEALOT field campaign. The maximum N₂O₅ mixing ratio was ∼100 pptv on 22 March (82), while ClNO₂ reached 80 pptv.

N₂O₅ mixing ratio over the full range of atmospheric concentrations than does the NO_3^- ion.

Figure 8 shows a subset of the time series of N₂O₅ and ClNO₂ mixing ratios measured by the UW-CIMS during the first portion of ICEALOT. On 22 March (DOY 82), the *RV Knorr* was traveling east-northeast exiting the Long Island Sound, and continued in this direction through 24 March. By 24 March, the *RV Knorr* was several hundred km off the North American Continent in the North Atlantic (∼45° N, 55° W). During this period, the prevailing wind direction was westerly to northwesterly at 5–10 m/s, suggesting these data represent sampling of aged continental airmasses. Our observations show concentration maxima were 10–100 pptv during this period, which on the one hand are significant, relative to previously predicted values of ClNO₂ (Pechtl and von Glasow, 2007), but also illustrate the low detection limits of this method. Most nights while within the Long Island Sound (data not shown), N₂O₅ reached 100–250 pptv on average during night, with average nighttime ClNO₂ being generally equal to or higher at mixing ratios of 150–200 pptv.

During the field deployment, several tests were performed to assess the presence of interferences at the *m/z* used to detect ClNO₂ and the potential generation of ClNO₂ by reactions of N₂O₅ on inlet tubing walls. Figure 9 summarizes the results of such tests. In the top panel, we plot the raw signal obtained at $I(^{35}ClNO_2)^-$ *m/z* versus the signal at the $I(^{37}ClNO_2)^-$ *m/z* from the entire period of sampling in the Long Island Sound (see Fig. 8). A linear least squares fit to the data (not shown), forced through the intercept, yields a slope of 0.3207 and R^2=0.996. This is within 0.5% percent of the theoretical isotopic value, 0.3199, indicated by the thick solid line. The experimental and theoretical values are well within the precision of the instrument
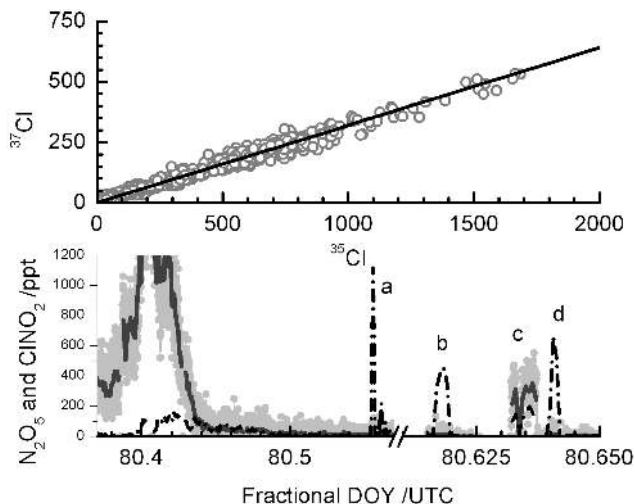

Fig. 9. Upper Panel: the measured ClNO₂ isotope ratio (open circles) and a linear fit (*m*=0.320, R^2=0.996). Lower Panel: time trace of N₂O₅ (black dashed line), ClNO₂ (grey) and 1-min binned average ClNO₂ (dark grey) mixing ratios for 20 March 2008. **(a)** Standard addition of 1.02 ppbv of N₂O₅ to the ambient sample flow. **(b)** Standard addition of ∼500 pptv of N₂O₅ to the ambient sample bypassing a wet NaCl salt bed. **(c)** Standard addition of ∼500 pptv of N₂O₅ to ambient sample flow which passes over the wet NaCl salt bed. **(d)** Standard addition of 700 pptv of N₂O₅ to the ambient sample flow bypassing the NaCl salt bed.

expected for 100 ms sampling. This result provides confidence that our measurements were of a chlorine-containing species that had the same *m/z* as ClNO₂ and can be destroyed on hot (450 K) stainless steel. We note that the signals detected at the ICl⁻ *m/z* did not demonstrate the expected Cl-isotopic ratio. The ICl isotope ratio was baised to the ³⁷Cl isotope, indicating an interfering unknown ion present at *m/z* 163.9 amu (I³⁷Cl⁻) which is not present at I³⁵Cl⁻. In the lower panel of Fig. 9, we show raw signals at the $I(N_2O_5)^-$ and the $I(^{35}ClNO_2)^-$ *m/z* during a standard addition of 2.0 ppbv N₂O₅ to ambient air. The N₂O₅ was added directly to the very top of the sampling manifold, 1cm from the sampling tip, just after a full night of continuous sampling and detection of N₂O₅ and ClNO₂. The first addition occurs at the point labeled "a". The N₂O₅ signal responds from a background count rate of 15 Hz to 2200 Hz, yielding a UW-CIMS calibration factor for N₂O₅ of 1.1 Hz/pptv in ambient air. No change in the ClNO₂ signal is evident during the N₂O₅ addition confirming that production of ClNO₂ from N₂O₅ reactions on the tubing wall was minimal during this, and most such additions. Indeed, while the sampling manifold was cleaned almost daily, we used any evidence of ClNO₂ signal enhancements during N₂O₅ additions to ambient air as an indication of inlet contamination and the inlet tubing was replaced and the sampling manifold was cleaned. Each fitting was washed in a distilled water/micropor soap solution using a sonicator. The fittings were then rinsed thoroughly and baked in an oven for several hours.

5 Summary and conclusions

We report on a new method for the simultaneous in situ detection of nitryl chloride, ClNO$_2$, and N$_2$O$_5$ using chemical ionization mass spectrometry (CIMS). The novel N$_2$O$_5$ detection scheme is direct and it does not suffer from high and variable chemical interferences, which are associated with the more typical nitrate anion based approach. We address the roles of water vapor, electric field strengths, and instrument zero determinations, which can greatly influence the overall sensitivity and detection limit of the method. The sensitivity to both N$_2$O$_5$ and ClNO$_2$ is logarithmically dependant on the partial pressure of water vapor in the ion-molecule reaction region. Under typical marine boundary layer conditions, the technique can be largely insensitive to changes in atmospheric water vapor concentrations, but under continental sampling, low water vapor concentrations could greatly reduce sensitivity. Detection of the iodide-clusters of these species has a threshold-dependence on the electric field strength in the CDC. Above -70 V/cm at 1.5 torr in the CDC, the clusters become essentially undetectable. We demonstrate the ability for simultaneous in situ measurements of ClNO$_2$ and N$_2$O$_5$ while on board the *R/V Knorr* as part of the ICEALOT 2008 Field Campaign. These observations serve to reinforce the importance of ClNO$_2$ as a nocturnal NO$_x$ and Cl-atom reservoir in coastal regions. Our technique allows a way to measure both reactant (N$_2$O$_5$) and product (ClNO$_2$) of complex gas-particle chemistry with a single instrument.

References

Aldener, M., Brown, S. S., Stark, H., Williams, E. J., Lerner, B. M., Kuster, W. C., Goldan, P. D., Quinn, P. K., Bates, T. S., Fehsenfeld, F. C., and Ravishankara, A. R.: Reactivity and Loss Mechanisms of NO$_3$ and N$_2$O$_5$ in a Polluted Marine Environment: Results from in situ Measurements during New England Air Quality Study 2002, J. Geophys. Res.-Atmos., 111, D23S73, doi:10.1029/2006JD007252, 2006.

Arsene, C., Bougiatioti, A., Kanakidou, M., Bonsang, B., and Mihalopoulos, N.: Tropospheric OH and Cl levels deduced from non-methane hydrocarbon measurements in a marine site, Atmos. Chem. Phys., 7, 4661–4673, 2007, http://www.atmos-chem-phys.net/7/4661/2007/.

Atkinson, R.: Atmospheric Chemistry of VOCs and NO$_x$, Atmos. Environm., 34, 2063–2101, 2000.

Ayers, J. D. and Simpson, W. R.: Measurements of N$_2$O$_5$ near Fairbanks, Alaska, J. Geophysi. Res.-Atmos., 111, D14309, doi:10.1029/2006JD007070, 2006.

Behnke, W., George, C., Scheer, V., and Zetzsch, C.: Production and Decay of ClNO$_2$ from the Reaction of Gaseous N$_2$O$_5$ with NaCl solution: Bulk and Aerosol Experiments, J. Geophys. Res.-Atmos., 102, 3795–3804, 1997.

Bertram, T. H., Thornton, J. A., and Riedel, T. P.: An experimental technique for the direct measurement of N$_2$O$_5$ reactivity on ambient particles, Atmos. Meas. Tech. Discuss., 2, 689–723, 2009, http://www.atmos-meas-tech-discuss.net/2/689/2009/.

Brown, S. S., Dube, W. P., Osthoff, H. D., Stutz, J., Ryerson, T. B., Wollny, A. G., Brock, C. A., Warneke, C., De Gouw, J. A., Atlas, E., Neuman, J. A., Holloway, J. S., Lerner, B. M., Williams, E. J., Kuster, W. C., Goldan, P. D., Angevine, W. M., Trainer, M., Fehsenfeld, F. C., and Ravishankara, A. R.: Vertical Profiles in NO$_3$ and N$_2$O$_5$ Measured from an Aircraft: Results from the NOAA P-3 and Surface Platforms during the New England Air Quality Study 2004, J. Geophys. Res.-Atmos., 112, D22304, doi:10.1029/2007JD008883, 2007.

Brown, S. S., Neuman, J. A., Ryerson, T. B., Trainer, M., Dube, W. P., Holloway, J. S., Warneke, C., de Gouw, J. A., Donnelly, S. G., Atlas, E., Matthew, B., Middlebrook, A. M., Peltier, R., Weber, R. J., Stohl, A., Meagher, J. F., Fehsenfeld, F. C., and Ravishankara, A. R.: Nocturnal Odd-Oxygen Budget and its Implications for Ozone Loss in the Lower Troposphere, Geophys. Res. Lett., 33, L08801, doi:10.1029/2006GL025900, 2006.

Brown, S. S., Stark, H., Ciciora, S. J., McLaughlin, R. J., and Ravishankara, A. R.: Simultaneous in situ Detection of Atmospheric NO$_3$ and N$_2$O$_5$ via Cavity Ring-Down Spectroscopy, Rev. Sci. Instrum., 73, 3291–3301, 2002.

Cavender, A. E., Biesenthal, T. A., Bottenheim, J. W., and Shepson, P. B.: Volatile organic compound ratios as probes of halogen atom chemistry in the Arctic, Atmos. Chem. Phys., 8, 1737–1750, 2008, http://www.atmos-chem-phys.net/8/1737/2008/.

Dentener, F. J. and Crutzen, P. J.: Reaction of N$_2$O$_5$ on Tropospheric Aerosols – Impact on the Global Distributions of NO$_x$, O$_3$, and OH, J. Geophys. Res.-Atmos., 98, 7149–7163, 1993.

Evans, M. J. and Jacob, D. J.: Impact of new Laboratory Studies of N$_2$O$_5$ Hydrolysis on Global Model Budgets of Tropospheric Nitrogen Oxides, Ozone, and OH, Geophys. Res. Lett., 32, L09813, doi:10.1029/2005GL022469, 2005.

Finlayson-Pitts, B. J., Ezell, M. J., and Pitts, J. N.: Formation of Chemically Active Chlorine Compounds by Reactions of Atmospheric NaCl Particles with Gaseous N$_2$O$_5$ and ClONO$_2$, Nature, 337, 241–244, 1989.

Fuchs, H., Dube, W. P., Cicioira, S. J., and Brown, S. S.: Determination of Inlet Transmission and Conversion Efficiencies for in situ Measurements of the Nocturnal Nitrogen Oxides, NO$_3$, N$_2$O$_5$ and NO$_2$, via Pulsed Cavity Ring-Down Spectroscopy, Anal. Chem., 80, 6010–6017, 2008.

Geyer, A., Alicke, B., Mihelcic, D., Stutz, J., and Platt, U.: Compar-

ison of Tropospheric NO$_3$ Radical Measurements by Differential Optical Absorption Spectroscopy and Matrix Isolation Electron Spin Resonance, J. Geophys. Res.-Atmos., 104, 26097–26105, 1999.

Harrison, A. G.: Chemical Ionization Mass Spectrometry, CRC Press, Boca Raton, FL, USA, 1983.

Heintz, F., Platt, U., Flentje, H., and Dubois, R.: Long-term Observation of Nitrate Radicals at the Tor Station, Kap Arkona (Rugen), J. Geophys. Res.-Atmos., 101, 22891–22910, 1996.

Huey, L. G.: Measurement of Trace Atmospheric Species by Chemical Ionization Mass Spectrometry: Speciation of Reactive Nitrogen and Future Directions, Mass Spectrom. Rev., 26, 166–184, 2007.

Huey, L. G., Hanson, D. R., and Howard, C. J.: Reactions of SF$_6^-$ and I$^-$ with Atmospheric Trace Gases, J. Phys. Chem., 99, 5001–5008, 1995.

Jacob, D. J.: Heterogeneous Chemistry and Tropospheric Ozone, Atmos. Environ., 34, 2131–2159, 2000.

Logan, J. A., Prather, M. J., Wofsy, S. C., and McElroy, M. B.: Tropospheric Chemistry – A Global Perspective, J. Geophys. Res., 86, 7210–7255, 1981.

McNeill, V. F., Patterson, J., Wolfe, G. M., and Thornton, J. A.: The effect of varying levels of surfactant on the reactive uptake of N$_2$O$_5$ to aqueous aerosol, Atmos. Chem. Phys., 6, 1635–1644, 2006, http://www.atmos-chem-phys.net/6/1635/2006/.

Mentel, T. F., Bleilebens, D., and Wahner, A.: A Study of Nighttime Nitrogen Oxide Oxidation in a Large Reaction Chamber - The Fate of NO$_2$ N$_2$O$_5$, HNO$_3$, and O$_3$ at Different Humidities, Atmos. Environ., 30, 4007–4020, 1996.

Noxon, J. F., Norton, R. B., and Marovich, E.: NO$_3$ in the Troposphere, Geophys. Res. Lett., 7, 125–128, 1980.

Osthoff, H. D., Roberts, J. M., Ravishankara, A. R., Williams, E. J., Lerner, B. M., Sommariva, R., Bates, T. S., Coffman, D., Quinn, P. K., Dibb, J. E., Stark, H., Burkholder, J. B., Talukdar, R. K., Meagher, J., Fehsenfeld, F. C., and Brown, S. S.: High Levels of Nitryl Chloride in the Polluted Subtropical Marine Boundary Layer, Nature Geoscience, 1, 324–328, 2008.

Pechtl, S. and von Glasow, R.: Reactive Chlorine in the Marine Boundary Layer in the Outflow of Polluted Continental Air: A Model Study, Geophys. Res. Lett., 34, L11813, doi:10.1029/2007GL029761, 2007.

Platt, U., Allan, W., and Lowe, D.: Hemispheric average Cl atom concentration from ^{13}C/^{12}C ratios in atmospheric methane, Atmos. Chem. Phys., 4, 2393–2399, 2004, http://www.atmos-chem-phys.net/4/2393/2004/.

Platt, U. and Heintz, F.: Nitrate Radicals in Tropospheric Chemistry, Israel J. Chem., 34, 289–300, 1994.

Simpson, W. R.: Continuous Wave Cavity Ring-Down Spectroscopy Applied to in situ Detection of Dinitrogen Pentoxide (N$_2$O$_5$), Rev. Sci. Instrum., 74, 3442–3452, 2003.

Slusher, D. L., Huey, L. G., Tanner, D. J., Flocke, F. M., and Roberts, J. M.: A Thermal Dissociation-Chemical Ionization Mass Spectrometry (TD-CIMS) Technique for the Simultaneous Measurement of Peroxyacyl Nitrates and Dinitrogen Pentoxide, J. Geophys. Res.-Atmos., 109, D19315, doi:10.1029/2004JD004670, 2004.

Smith, N., Plane, J. M. C., Nien, C. F., and Solomon, P. A.: Nighttime Radical Chemistry in the San-Joaquin Valley, Atmos. Environ., 29, 2887–2897, 1995.

Spicer, C. W., Chapman, E. G., Finlayson-Pitts, B. J., Plastridge, R. A., Hubbe, J. M., Fast, J. D., and Berkowitz, C. M.: Unexpectedly High Concentrations of Molecular Chlorine in Coastal Air, Nature, 394, 353–356, 1998.

Stutz, J., Alicke, B., Ackermann, R., Geyer, A., White, A., and Williams, E.: Vertical Profiles of NO$_3$, N$_2$O$_5$, O$_3$, and NO$_x$ in the Nocturnal Boundary Layer: 1. Observations during the Texas Air Quality Study 2000, J. Geophys. Res.-Atmos., 109, D12306, doi:10.1029/2007JD008883, 2004.

Thornton, J. A. and Abbatt, J. P. D.: N$_2$O$_5$ Reaction on Submicron Sea Salt Aerosol: Kinetics, Products, and the Effect of Surface Active Organics, J. Phys. Chem. A, 109, 10004–10012, 2005.

Thornton, J. A., Braban, C. F., and Abbatt, J. P. D.: N$_2$O$_5$ Hydrolysis on Sub-Micron Organic Aerosols: the Effect of Relative Humidity, Particle Phase, and Particle Size, Phys. Chem. Ch. Ph., 5, 4593–4603, 2003.

van Aardenne, J. A., Carmichael, G. R., Levy, H., Streets, D., and Hordijk, L.: Anthropogenic NO$_x$ Emissions in Asia in the Period 1990–2020, Atmos. Environ., 33, 633–646, 1999.

Veres, P., Roberts, J. M., Warneke, C., Welsh-Bon, D., Zahniser, M., Herndon, S., Fall, R., and de Gouw, J.: Development of Negative-Ion Proton-Transfer Chemical-Ionization Mass Spectrometry (NI-PT-CIMS) for the Measurement of Gas-Phase Organic Acids in the Atmosphere, Int. J. Mass Spectrom., 274, 48–55, 2008.

Wayne, R. P., Barnes, I., Biggs, P., Burrows, J. P., Canosamas, C. E., Hjorth, J., Lebras, G., Moortgat, G. K., Perner, D., Poulet, G., Restelli, G., and Sidebottom, H.; The Nitrate Radical - Physics, Chemistry, and the Atmosphere, Atmos. Environ. A-Gen., 25, 1–203, 1991.

Wolfe, G. M., Thornton, J. A., McNeill, V. F., Jaffe, D. A., Reidmiller, D., Chand, D., Smith, J., Swartzendruber, P., Flocke, F., and Zheng, W.: Influence of trans-Pacific pollution transport on acyl peroxy nitrate abundances and speciation at Mount Bachelor Observatory during INTEX-B, Atmos. Chem. Phys., 7, 5309–5325, 2007, http://www.atmos-chem-phys.net/7/5309/2007/.

Wood, E. C., Wooldridge, P. J., Freese, J. H., Albrecht, T., and Cohen, R. C.: Prototype for in situ detection of Atmospheric NO$_3$ and N$_2$O$_5$ via Laser-Induced Fluorescence, Environ. Sci. Technol., 37, 5732–5738, 2003.

Yienger, J. J.: An Evaluation of Chemistry's Role in the Winter-Spring Ozone Maximum found in the Northern Midlatitude Free Troposphere, J. Geophys. Res.-Atmos., 104, 8329–8329, 1999.

Zhu, R. S. and Lin, M. C.: ab initio Studies of ClOx Reactions: Prediction of the Rate Constants of ClO+NO for the Forward and Reverse Processes, Chem. Phys. Chem., 5, 1864–1870, 2004.